e-ISSN 2320 –7876 www.ijfans.org
Vol.11, Iss.9, Dec 2022

Research Paper

RETINAL IMPLANTS:FRACTAL ELECTRODES FOR INTERFACING NEURONS.PARAMETER ESTIMATION AND QUANTUM STATE:ERROR MODEL

GOPINATHAN.N
Research Scholar
M.Phil Physics
Bharath Institute Of Higher Education And Research
Mail Id : ngntamil@rediffmail.com

Dr.K.THIYAGARAJAN
Head of the Department, Department Of Physics
Bharath Institute Of Higher Education And Research

Address for Correspondence

GOPINATHAN.N
Research Scholar
M.Phil Physics
Bharath Institute Of Higher Education And Research
Mail Id : ngntamil@rediffmail.com

INTRODUCTION:

The retina is the innermost layer of the eye occupying the posterior two-third of the eye.It is a layer of photosensitive cells concerned with initial processing of visualinformation. The sensation of sight is based on a step-wise process in which light isfocused on the retina, converted to electrical impulses that are conveyed through thevisual pathways to the visual cortex of the brain where it is interpreted as a visual signal. The neurons in the retina are broadly of three types. (1) the photoreceptors, whichare located the most externally, (2) the intermediate neurons (3) the ganglion cells.

Major types of cells of the retina

Photoreceptors Rods and cones are the two types of photoreceptor cells present in the retina. Rodsmediate dim light vision, whereas cones function in bright light. Rods provide

sensitivity to scotopic (dim light) vision whereas cones provide visual acuity for pattern detection and color vision. All the photoreceptors have an outer segment that contains the visualpigment and an inner segment which contains the nucleus.

In histologic sections, the retina is seen to consist of ten layers (shown in Fig 1.1).

The outermost layer is the retinal pigment epithelium (RPE), consisting of melanin granules which help in the absorption of scattered light and increase the efficiency of photoreceptors. The RPE also acts as blood retinal barrier, helps in transport of nutrients, is essential for metabolism of vitamin A derivatives, and performs phagocytosis of outer segments of rods and cones. Inner to the RPE is the layer of rods and cones, which consists of the photoreceptor outer and inner segments. The outer segments contain visualpigment and function in phototransduction, while the inner segment contains theirmetabolic machinery i.e the nucleus and dense aggregation of mitochondria. The externallimiting membrane is adjacent to the photoreceptor inner segments and is formed by theMuller cell tight junction connections with the photoreceptors. The next layer consistsofthe outer nuclear layer, which is formed by the nuclei of rods and cones. Inner to theouter nuclear layer is the outer plexiform layer, containing synapses between thephotoreceptors and horizontal and bipolar cells. Interior to this is the inner nuclear layer,containing the nuclei and cell bodies of bipolar cells, horizontal cells and mullercells,followed by the inner plexiform layer, which is made up of synapses between bipolar,amacrine and ganglion cells. The innermost cell layer is the ganglion cell layer, whichconsists of cell bodies of ganglion cells. Inner to this is the nerve fiber layer, whichconsists of the axons of ganglion cells. The innermost layer of retina is the internallimiting membrane, formed by the projections of the Muller cells (Blanks *et al*., 1994).

e-ISSN 2320 –7876 www.ijfans.org
Vol.11, Iss.9, Dec 2022

Research Paper

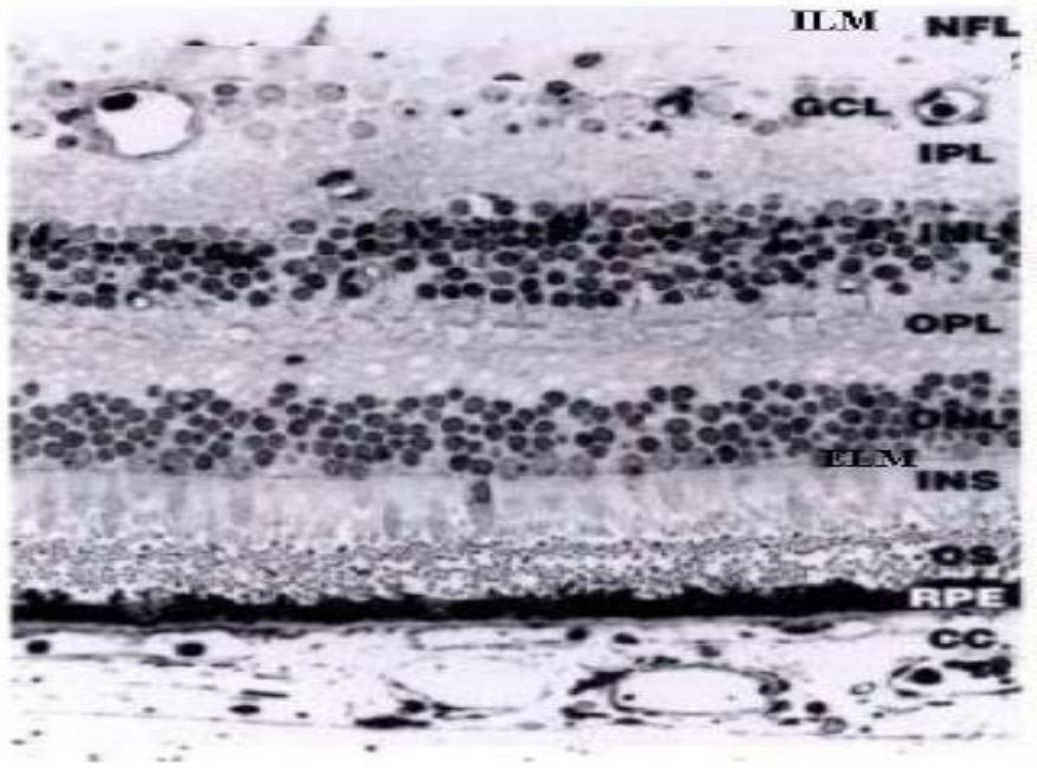

Figure 1.1: Section of the human retina showing the different layers. From the inner to the outer retina, these are- internal limiting membrane (ILM), nerve fiber layer (NFL), ganglion cell layer (GCL), inner plexiform layer (IPL), inner nuclear layer (INL), outer plexiform layer (OPL), outer nuclear layer (ONL), external limiting membrane (ELM), inner segments (INS) and outer segments (OS) of the photoreceptors, retinal pigment epithelium (RPE), choriocapillaris (CC) (Picture taken from Forrester *et al*., 2001).

Retinal differentiation

Differentiation of photoreceptors in the retina of various species has been studied and ithas been found that in all the vertebrates the cone photoreceptors are generated before the rod photoreceptors (Levine *et al*., 2000). *In vitro* experiments with chick embryo tissue destined to form retinal progenitor cells have suggested that cones are not dependent on the surrounding cells for differentiation, while the differentiation of rods *in vitro* requires a critical cell density suggesting a requirement of signaling molecules from surrounding cells. Some of the factors that promote rod photoreceptor differentiation are hedgehog factors, activin, retinoic acid, ciliaryneurotrophic factor and fibroblast growth factor (Levine *et al*., 2000).

e-ISSN 2320 –7876 www.ijfans.org
Vol.11, Iss.9, Dec 2022

Differentiation of the inner retina starts immediately after the final mitotic division at their ventricular surface. Retinal cells then migrate to their appropriate lamina.As they migrate, the different types of neuron begin to take on some morphologicalfeatures of their characteristic cell type. For example, ganglion cells begin to elongatetheir axon before the point when their lamina reaches the ganglion cell layer. The nextphase in the differentiation of retinal neurons is the growth of dendritic processes. In thelast stages of differentiation the retinal neurons make morphologically identifiablesynapses with one another and express their transmitters and receptors. The time courseof these events overlaps considerably (Reh*et al*., 2001).

Retinal maturation

As the retina matures, nearly all the events continue to proceed in a central to peripheral direction. Once the process of retinal histogenesis is complete, remodeling continues primarily in the form of retinal stretch, owning to steadily increasing intraocular pressure. The development of the fovea in primates is another aspect of later retinal development (Reh*et al*., 2001).

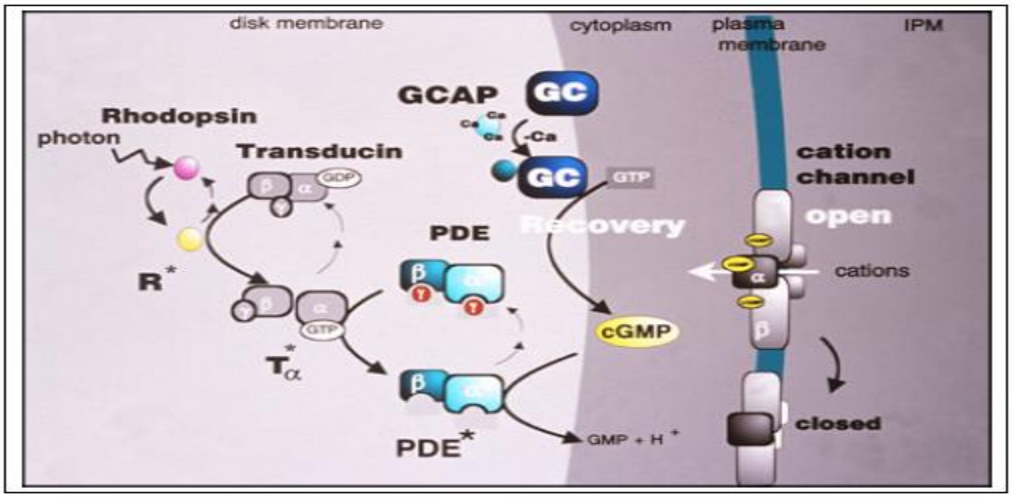

Visual cycle

The visual cycle comprises a series of enzymatic reactions that help in the regeneration of 11-cis retinal from all-trans retinal. The process of vision begins with the photoisomerization of visual pigment chromophore 11-cis retinal to all-trans retinal. For opsin to function in vision, it must reunite with another 11-cis retinal molecule to produce rhodopsin or cone opsins. But neither rods nor cones can regenerate 11-cis retinal without the involvement of other ocular cells (Mata et

al., 2002). The regeneration of 11-cis retinal is accomplished by the cycling of vitamin A analogs between the photoreceptors and retinal pigment epithelium, in case of rods (Randoet al., 2001) which is well accepted, and recently it has been proposed (Calvert et al., 1995) that in case of cones the Muller cells are involved in the regeneration of 11-cis retinal (Figure 1.5).

Visual cycle in rods

On absorption of light by rhodopsin, the chromophore of rhodopsin, 11-cis retinal, gets isomerised to all-trans retinal. All-trans retinal formed after photoisomerizationeventually gets detached from opsin, as a result photochemically inactive opsin and alltranretinal are formed. For opsin to function again in vision, it must reunite with molecule of 11-cis retinal, to form a rhodopsin molecule. The all-trans retinal is short lived in photoreceptors, as it is chemically highly reactive (Lamb et al., 2004), and is rapidly reduced to all-trans retinol by alcohol dehydrogenase enzyme (RDH12) in the photoreceptor outer segments. All-trans retinol (vitamin A) thus formed leaves the photoreceptor outer segment and is transported to retinal pigment epithelium (RPE) by interphotoreceptor retinoid-binding protein (IRBP), which is found in the interphotoreceptor space. On entry to the RPE all-trans retinol is recognized by cellular retinol binding protein (CRBP), which is highly specific for binding to all-trans retinol incomparison to other isomers including 11-cis retinol (Lamb et al., 2004). Next the alltransretinol is esterified to all-trans retinyl esters in the presence of lecithin retinol acyl transferase (LRAT) enzyme by transferring the acyl group of lecithin to all-trans retinol. All-trans retinyl esters formed are then isomerized and hydrolyzed to 11-cis retinol by as single enzyme called isomerohydrolase/RPE65 (Moiseyevet al., 2005). The final step in the generation of chromophore is the oxidation of 11-cis retinol to 11-cis retinal by 11-cisretinol dehydrogenase enzyme (RDH5) (Simon et al.,1999). The 11-cis retinal regenerated in the RPE is transported to the outer segments of the photoreceptor through IRBP and the bleached opsin is regenerated and the rod visual cycle is completed (Figure 1.5) (Carlson et al., 1992, Randoet al., 2001).

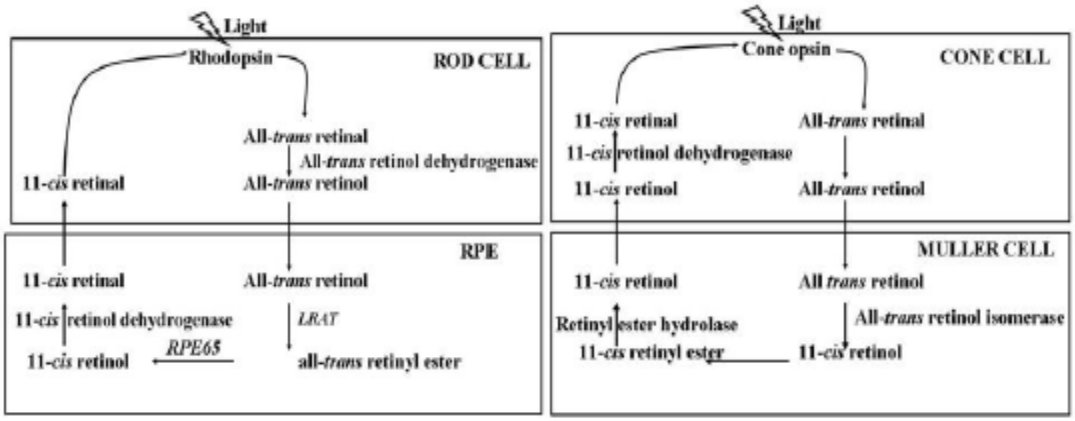

Figure 1.5. Schematic of visual cycle in rods (left) and cones (right). (Schematic drawn by taking the concept form Rando *et al*., 2001, Mata *et al*., 2002)

Visual cycle in cones

Through experiments on the retinas of cone-dominated animals (chicken and groundsquirrel) Mata and coworkers (2002), have proposed that the cones regenerate their visual pigment by using Muller cells. Apart from similarities with the rod visual cycle, visual pigment regeneration in cones shows three catalytic activities, as shown in Figure 1.5 (Mata et al., 2002). The all-trans retinol generated in the cones is transported to the Muller cells, where all-trans retinol is isomerized to 11-cis retinol by all-trans retinol isomerase in the presence of palmitoyl coenzyme A. The 11-cis retinol formed is converted to 11-cis retinyl ester by a second enzyme called 11-cis retinyl ester synthase which is distinct from lecithin retinol acyltransferase (LRAT) (Mata *et al*., 2002). This enzyme catalyses

the formation of 11-*cis* retinyl esters but not the all-*trans* retinyl esters. The11-*cis* retinylester is then converted to 11-*cis* retinol by retinyl ester hydrolase enzyme, and is transported to the cones by interphotoreceptor retinoid-binding protein (IRBP). In the cones 11-*cis* retinol is converted to 11-*cis* retinal by 11-*cis* retinol dehydrogenase. This dehydrogenase is different from the enzyme of the rod visual cycle in that it uses NADP+ as cofactor (Mata *et al*., 2002), while 11-*cis* retinol dehydrogenase of the rod visual cycle uses NAD+ as cofactor (Jang *et al*., 2000). The 11-*cis* retinal is used to regenerate the coneopsins, and the cone visual cycle is completed.

Retinal dystrophies

Retinal dystrophies are a group of disorders characterized by inherited, progressive dysfunction, cell loss and eventual atrophy of retinal tissue. Retinal dystrophies are heterogeneous both

genetically and clinically and involve primarily the degeneration of photoreceptors. They are classified according to the type of photoreceptor (rod or cone) primarily involved and on the mode of inheritance. Further, in certain forms, there are manifestations of disease that are restricted to the retina (non-syndromic) or involve dysfunction of other organs apart from the eye (syndromic). The involvement of both rods and cones in advanced stages of disease in several of these disorders may make them clinically indistinguishable.

Classification

Retinal dystrophies can be broadly classified into following types:

1. Rod and rod-cone dystrophies
2. Cone dystrophies
3. Macular dystrophies
4. Leber congenital amaurosis

Rod and rod-cone dystrophies

Rod and rod-cone dystrophies include those retinal dystrophies which primarily involve the degeneration of rod photoreceptors. Loss of rod photoreceptors can be progressive or non-progressive. The progressive forms are termed rod-cone types as loss of rod cells eventually lead to loss of cone photoreceptors, while in the non-progressive forms, only rod cells are lost.

INTEGRATED RETINAL IMPLANTS

Outer retinal diseases Age related macular degeneration (AMD) and retinitis pigmentosa (RP) are two of the most common outer retinal degenerative diseases that result in human vision impairment and blindness. According to the World Health Organization (WHO), AMD has become the third leading cause of blindness on global scale, and ranks first in developed countries [1]. In fact, it has been estimated that almost 3 million people in the United States will have significant symptoms associated with AMD by 2020 [2]. As for RP, it has affected more than 500,000 people in the United States, among whom 20,000 are legally blind [3]. AMD primarily affects the central vision regions in people age 60 and older (Figure 2.1 (b)). Because the brain will compensate for central dark patches during its early stages, it is difficult to diagnose this disease until the advanced stages. Whereas for patients with RP, vision deterioration develops gradually and progressively, starting from defective dark adaptation (night blindness), followed

by the reduction of peripheral vision (known as tunnel vision in Figure 2.1 (c)), and, sometimes, a complete vision loss in the advanced stages of the disease [4].

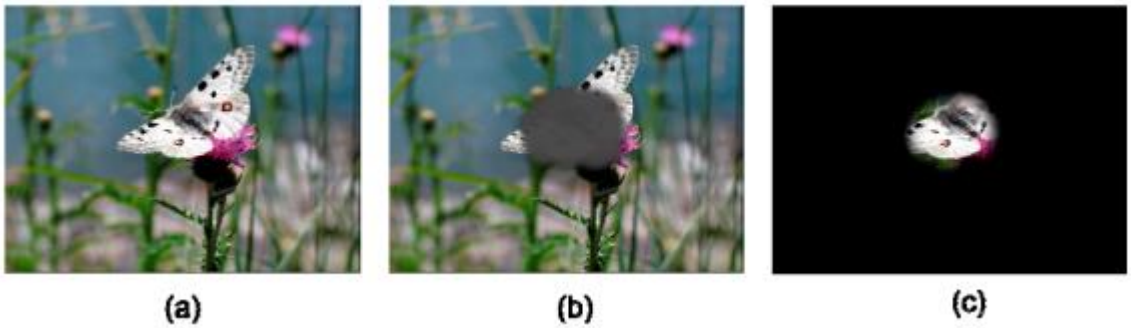

Figure 2.1: (a) Normal vision. (b) Loss of central vision in patients with AMD. (c) Tunnel vision in patients with RP. (Images courtesy of Artificial Retina Project)

Although the mechanisms of these retinal diseases are not fully understood, histopathological studies indicate they are mainly restricted to outer retinal region, and associated with the damage of photoreceptor cells [5-8]. The photoreceptor cells (rods and cones) are situated in a deep retinal layer, and they, along with other cells (bipolar, ganglion, horizontal and amacrine cells), perform significant visual processing and communication tasks in normal vision (Figure 2.1). In a healthy retina, particularly, the photoreceptors initiate neural responses to incoming light by converting light into chemical and electrical signals. The bipolar and ganglion cells in the inner retina then pass the visual signals toward the optic nerve. Along the way, the horizontal and amacrine cells provide lateral interaction between neighboring cells [9].

Current treatments for such retinal degenerative diseases rely on gene replacement therapy, pharmaceutical therapy, nutritional therapy and dietary to slow down the development of blindness in their early stages [10, 11]. Nevertheless, once the vision is completely lost, no effective treatment exists that can cure these diseases. Studies on animal models show that photoreceptor and stem cell transplantations could be possible treatments by replacing the damaged retinal cells [12, 13]. However, they are still in development, and not yet ready for clinical practice. Other concerns such as expensive costs and political issues also add barriers to their implementation. An alternative approach is proposed as bioelectronic visual prostheses, which bypass the damaged photoreceptor cells and utilize electrical stimulating to restore vision.

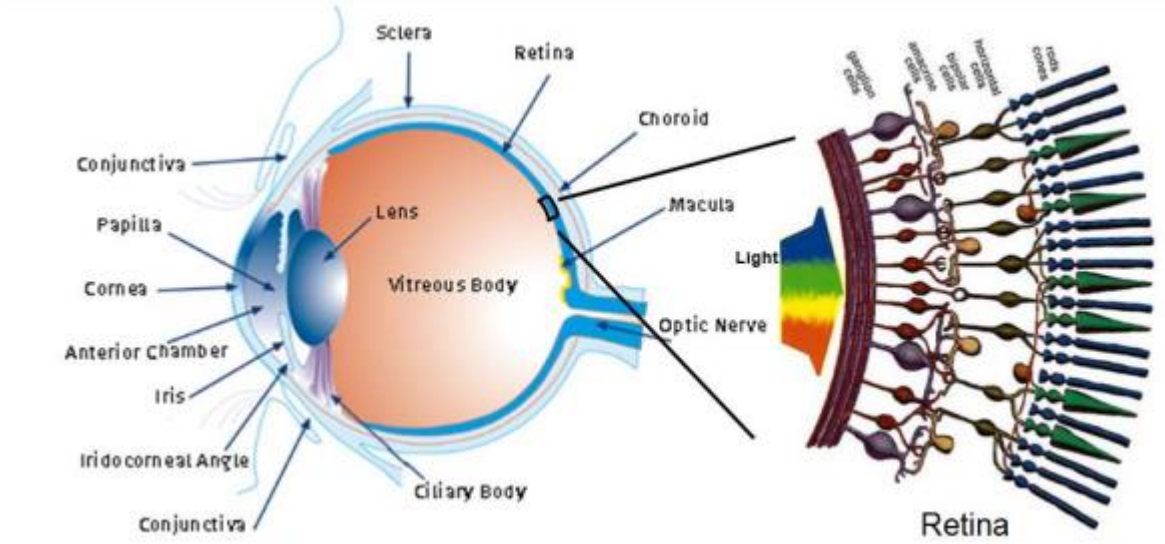

Figure 2.2: Horizontal cross section through human eye and the cell layers in the retina. (Eye illustrate adapted from Bausch & Lomb)

Artificial visual prostheses for AMD and RP treatments

IMPLANTABLE RF-COILED CHIP INTEGRATION TECHNOLOGY

Despite successful device development, a significant hindrance to the future progress of the retinal project is system integration, which demands high lead-count interconnects and hermetic packaging without compromising flexibility and biocompatibility. Traditional packaging technologies which use wire-bonding, flip chip, and tape automated bonding do not meet these requirements due to their low reliability, non-biocompatibility, and high fabrication costs. A MicroFlex interconnection (MFI) technology has been developed [85], in which flexible polyimide substrates are fabricated as carriers, and individual devices are mounted to the polymer substrates using bumpbonding method. While devices packaged with this technology are flexible enough, their long term biocompatibility has not been fully proven. Its tedious and low yield process also makes it difficult and costly to integrate high electrode density devices.

Accelerated-lifetime soaking test of Parylene protected ICs

Before delving into the integration technology, it is important to study the Parylene sealing performance on IC circuitry. To do that, similar ALSTs are performed on Parylene-protected IC chips. An EM4100 read-only radio-frequency identity (RFID) chip (EM Microelectronic, Switzerland) is used as a sample chip. This chip is a CMOS integrated circuit with metal

composition of Al-Ni-Au on contact pads. It can be powered up using an external coil with an electromagnetic field. By turning the modulation current on and off, the chip sends back a 64-bit sequence stored in the memory array. The operation frequency of the chip is between 100 kHz and 150 kHz, with 125 kHz being typical .

Unpowered soaking test is first performed in saline at 77 ºC. Samples are prepared by cleaning chips with isopropanol and DI water, followed by a Parylene C deposition of approximately 10 μm. Bare chips without Parylene coating are also tested as comparisons. During the soaking period, the samples are examined daily under a microscope. The test lasts up to six months, and then the samples are removed from hot saline for functionality measurement using a Wentworth Labs 11PO900 probe station (Wentworth Laboratories, Inc., Brookfield, CT, USA). As can be seen from Figure 3.1, the chip without Parylene coating experiences serious metal corrosion after only 2 days of soaking, while the samples with Parylene protection has not observable metal damage even after six months of soaking. Functionality test is performed on the Parylene coated chip after removing the Parylene on contact pads with oxygen plasma etching or probe tip scratching. The result shows that the chip is still well functioning, indicating that IC circuits can remain intact in hot saline for six months with Parylene protection.

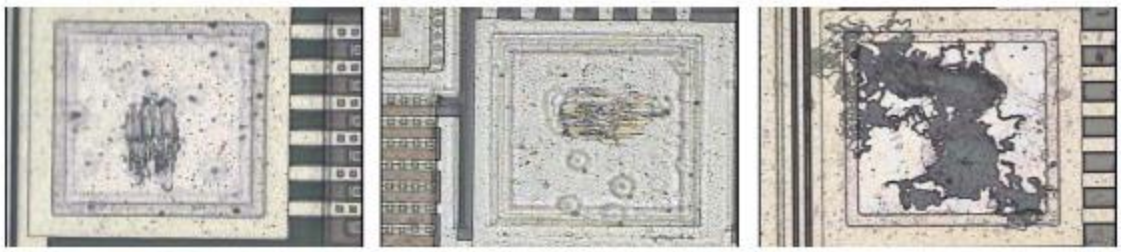

Figure 3.1: Microscope images of chip metal pads. (a) A chip coated with annealed Parylene C. (b) A chip with regular Parylene C after 6 months of soaking. (c) A bare chip after 2 days of soaking.

Given this exciting result, active soaking tests are conducted to further investigate the lifetime of the Parylene protected chip under continuous electrical stressing. In this case, the RFID chip is glued onto a Parylene cable using a biocompatible silver epoxy EPO-TEK H20E (Epoxy Technology, Billerica, MA, USA). The epoxy is fully cured and outgassed in a convection oven for 3 hours at 80 ºC. Regular wires are also pasted on the other side of the Parylene cable in order

e-ISSN 2320 –7876 www.ijfans.org
Vol.11, Iss.9, Dec 2022

to connect the chip to external test units, as shown in Figure 3.2. The device is then conformally coated with Parylene C for testing.

The soaking test is performed in a convection oven. During the test, the device is held in a glass bottle filled with regular saline, and the wires are connected to an external coil. The external hand-wound coil has an inductance of ~5.3 mH and an ESR of 88 Ω at 125 kHz. A commercially available RFID reader module (Parallax Inc. Rocklin, CA USA) is used to continuously send power and requests (24 hours a day) to the RFID chip though inductive coupling. The reader module contains an integrated coil with dimensions of 60 mm by 66mm, and is driven by a 5 volt DC supply. The output port of the reader is connected to an HP 54503A oscilloscope and a webcam is used to monitor the signal readout by taking a picture every 10 minutes (Figure 3.3).

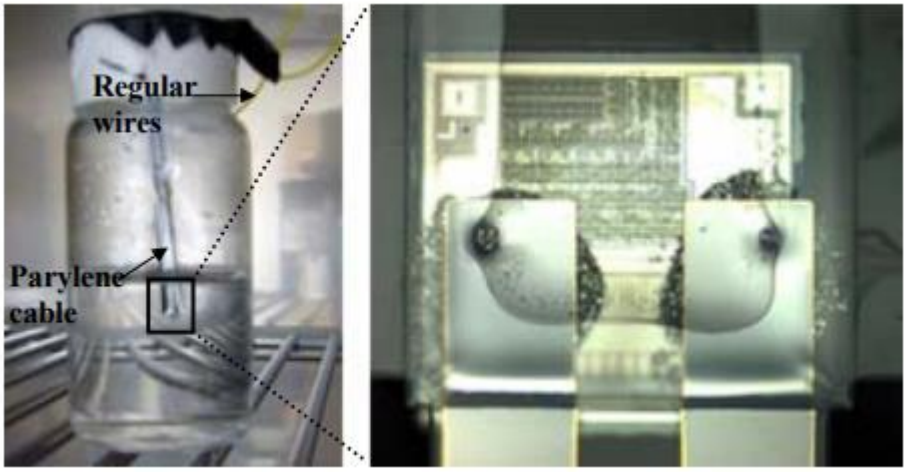

Figure 3.2: (left) Assembled RFID chip soaked in saline. (right) Close-up image of the attached RFID chip.

e-ISSN 2320 –7876 www.ijfans.org
Vol.11, Iss.9, Dec 2022

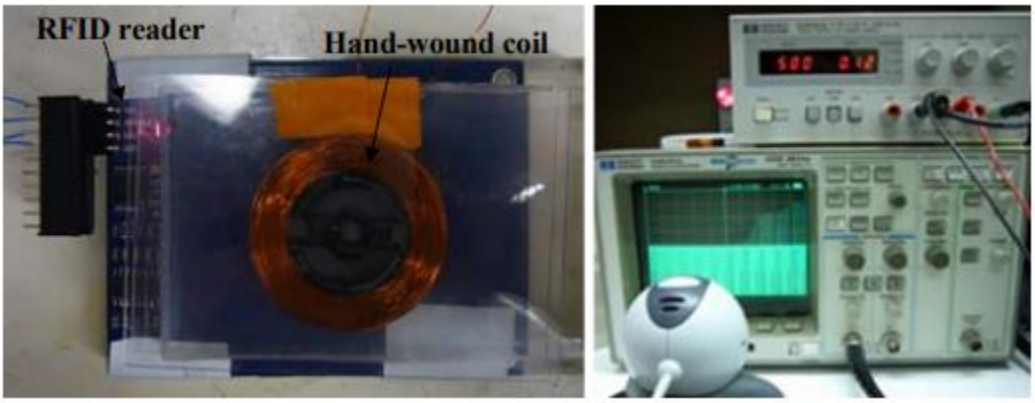

Figure 3.3: Test setup for the active soaking test of RFID chips.

Samples coated with different thicknesses of Parylene are tested at various temperatures. MTTF is defined as the time point when no output signal can be detected. Four samples are tested under each condition, and their MTTF and the standard deviation is plotted in Figure 3.4. According to the Arrhenius relationship, chips with 22.1 µmParylene coating will have an MTTF of ~ 2 years at 37°C under the active condition. Ideally, samples with thicker Parylene coating should have better durability if failure is solely caused by water permeation through Parylene. However, the results show that samples with 22.1 µmParylene coating do not show much advantage, indicating that other failure mechanisms besides water permeation might have taken place.

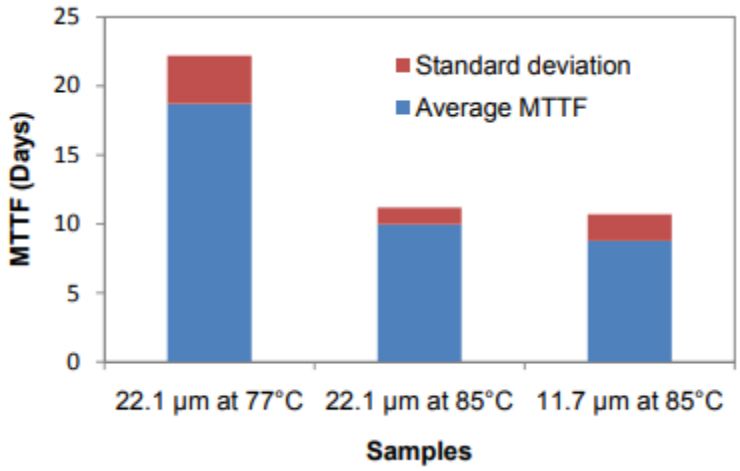

Figure 3.4: Active soaking test results of Parylene protected IC chips.

To find out the exact failure mode, the failed samples are examined using SEM. Parylene cracks are observed in samples with both 22.1 μm and 11.7 μmParylene C coatings. The mechanism of Parylene cracking has not been fully understood. It is possible that the chip generates a lot of heat under intensive electrical stress so that thermal stress concentrates along the edges due to poor heat dissipation. Also, it is noted that the test temperatures are very close to or within the range of the glass transition temperature of Parylene C (80 °C – 100 °C),therefore Parylene might undergo material property changes due to the recrystallization of the polymer chains. The active soaking test is still ongoing, and more experimental results are expected to enable a complete understanding of Parylene packaging behaviors.

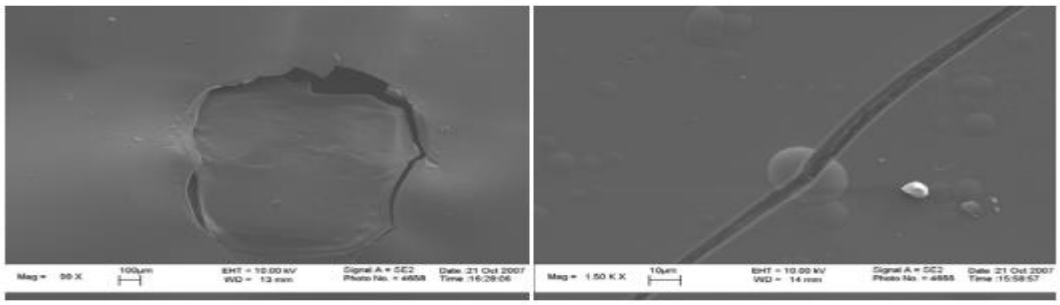

Figure 3.5: Parylene cracks is sample with (left) 11.7 μmParylene coating and (right) 22.1 μmParylene coating

The surgical implantation indicates that the modified design results in a better surgical outcome, and that the haptics significantly help the coil region to anchor within the angles. However, serious inflammation is observed in both eyes a week after implantation, which is probably caused by toxins released from the epoxy. To further address this matter, the epoxy needs to fully cure and outgas before implantation. A thicker Parylene coating on the epoxy will also improve the isolation of the epoxy from eye environment.

CONCLUSION

Two blindness diseases due to outer retinal degeneration are described in this chapter. Research shows that the visual prosthesis technology has great potential for treating these diseases and restoring the lost vision function. Four visual implantation approaches are discussed, among which the epiretinal retinal prosthesis has distinct advantages over others. However, a number of obstacles still exist, mainly related to material choice and fabrication development. Therefore, an

all-intraocular epiretinal implant system is proposed to address these issues, utilizing Parylene-based MEMS technologies for device fabrication and system integration.

Branched fractal electrodes best balance a number of competing requirements necessary for efficient neural stimulation from photodiode implants. (1) The gaps between the branches transmit large amounts of light into the underlying photodiode, thereby generating high electrode voltages. (2) The sidewalls of the branches create a large surface area and therefore a high electrode capacitance. For a given voltage, the fractal electrode then holds a large amount of charge and the electric field generated by this charge extends vertically far into the extracellular space. (3) The gaps ensure that, for a given covering area, the fractal has a large bounding area. By carefully selecting the optimal *D* and number of iterations, the field penetrates the gaps and ensures a uniform field that extends far laterally. Combined, the above factors ensure a large uniform field that penetrates a sufficient volume of extracellular space to maximize neural stimulation.

Consequently, the 20 μm fractal implant stimulates all of the surrounding bipolar neurons using 74% less irradiance compared to the square. In addition to an improved efficiency, the fractal's decreased threshold irradiance holds important consequences for the safe operation of future implants. For long-term continuous operation of implants, the square is just barely within the maximum permissible exposure limit while the fractal is significantly within. Moreover, for equivalent irradiance of 12 mW/mm^2 illuminating the best optimized square and fractals, the fractal stimulates ~90% more neurons. Thus, whereas the 20 μm fractal implant has the potential to deliver a maximum of 20/80 vision acuity, the square suffers a significant decrease in perceived image quality. When the performance factors reported here are coupled with potentially beneficial adhesive and mechanical properties, it is clear that fractal electrodes have the potential to dramatically improve the restored visual acuity from subretinal implants.

The electrical properties of MEMS receiver coils, including self-inductance, ESR, and parasitic capacitance, are predicted with respect to the coil geometries using analytic models. The calculation values are consistent with the simulation results in CoventorWare. We have also studied a simplified inductive link to evaluate the power transfer capability of MEMS coils. The result indicates that a higher Q factor will improve the transfer efficiency and overall efficiency of the inductive link. Due to the nonlinear nature of the system, more accurate analysis may be needed in the future to simulate the circuit characteristics under nonlinear conditions using SPICE [67].

Nevertheless, the theoretical analysis above provides us a better understanding of the parasitic effects of the MEMS coil, and gives us the possibility to optimize the coil geometries to achieve maximum power transfer efficiency.

We have designed and successfully fabricated two types of MEMS coils using the Parylene-metal-Parylene skin technology. Experiments have been done to measure the electrical properties of the coils, which show good agreement with the theoretical values. The data transfer effect has been demonstrated at UCSC using the MEMS coil. However, the power transfer efficiency at a separation distance of 15 mm is below 0.5%, which is too low for high-density retinal stimulation. The most effective way to enhance the coil Q 88 factor is to increase the number of metal layers. While direct fabrication could be too complicated to carry out, the fold-and-bond technology has proven itself as a very promising alternative.

In this chapter, an embedded chip integration technology has been developed and successfully demonstrated by integrating a flexible Parylene RF coil with a commercially available read-only RFID chip. The functionality of the embedded chip is tested using an RFID reader module. Preliminary accelerated-lifetime passive soak testing has also been done in hot saline, which shows positive results for bioimplant packaging using Parylene. In addition, a neural stimulator, which features a single channel stimulation capability, hasbeen designed and the first prototype of the integrated system has been fabricated and tested to demonstrate its stimulation function in vitro.

REFERENCE

1. World Health Organization, "Magnitude and causes of visual impairment," http://www.who.int/medicacentre/factsheets/fs282/en/. (accessed: Aug. 26, 2008)

2. The Eye Diseases Prevalence Research Group, "Prevalence of age-related macular degeneration in the United States," Arch Ophthalmol, vol. 122, pp. 562-572, 2004.

3. Artificial Retina. Project, "Retinal diseases: Age-Related Macular Degeneration and Retinitis Pigmentosa," http://artificialretina.energy.gov/diseases.shtml. (accessed: Aug. 26,2008)

4. Wikipedia, "Retinitis pigmentosa." http://en.wikipedia.org/wiki/Retinitis pigmentosa. (accessed: Aug. 26, 2008)

5. W.R. Green and C. Enger, "Age-related macular degeneration histopathologic studies," The 1992 Lorenz E. Zimmerman Lecture. Ophthalmology, vol. 100, pp. 1519-1535, 1993.

6. F.H. Verhoeff, "Microscopic observations in a case of retinitis pigmentosa," Arch. Ophthalmol., vol. 5, pp. 392-407, 1931.

7. E.L. Berson, "Retinitis pigmentosa," Invest. Ophthalmol. Vis. Sci., vol. 34, pp. 1659-1676, 1993.

8. C.A. Curcio, N.E. Medeiros, and C.L. Millican, "Photoreceptor loss in age-related macular degeneration," Invest. Ophthalmol. Vis. Sci., vol. 37, pp. 1236-1249, 1996.

9. K.W. Horch and G.S. Dhillon, Neuroprosthetics Theory and Practice (Series on Bioengineering & Biomedical Engineering-Vol.2): World Scientific, 2004.

10. E.W.D. Norton, M.F. Marmor, D.D. Clowes, J.W. Gamel, C.C. Barr, A.R. Fielder, J. Marshall, E.L. Berson, B. Rosner, M.A. Sandberg, K.C. Hayes, B.W. Nicholson, C. Weigel-DiFranco, W. Willett, J.S. Felix, and A.M. Laties, "A randomized trial of vitamin A and vitamin E supplementation for retinitis pigmentosa," Arch. Ophthalmol., vol. 11, pp. 1460-1466, 1993.

11. J. Bennett, T. Tanabe, D. Sun, Y. Zeng, H. Kjeldbye, P. Gouras, and A.M. Maguire, "Photoreceptor cell rescue in retinal degeneration (rd) mice by in vivo dene therapy," Nature Medicine, vol. 2, pp. 649-654, 1996.

12. V. Tropepe, B.L.K. Coles, B.J. Chiasson, D.J. Horsford, A.J. Elia, R.R. Mclnnes, and D.V.D. Kooy, "Retinal stem cells in the adult mammalian eye," Science, vol. 287, pp. 2032-2036, 2000.

13. R.E. MacLaren, R.A. Pearson, A. MacNeil, R.H. Douglas, T.E. Salt, M. Akimoto, A. Swaroop, J.C. Sowden, and R.R. Ali, "Retinal repair by transplantation of photoreceptor precursors," Nature, vol. 444, pp. 203-207, 2006.

14. G.S. Brindley and W.S. Lewin, "The senstaion produced by electrical stimulation of the visual cortex," J. Physiol., vol. 196, pp. 479-493, 1968.

15. W.H. Dobelle and M.G. Mladejovsky, "Phosphenes produced by electrical stimulation of human occipital cortex, and their application to the development of a prosthesis for the blind.," J. Physiol., vol. 243, pp. 553-576, 1974.

16. W.H. Dobelle, "Artificial vision for the blind by connecting a television camera to the brain," ASAIO J., vol. 46, 2000.

17. R.A. Normann, E.M. Maynard, P.J. Rousche, and D.J. Warren, "A neural interface for a cortical vision prosthesis," Vision Res., vol. 39, pp. 2577-2587, 1999.

18. D.R. Kipke, R.J. Vetter, J.C. Williams, and J.F. Hetke, "Silicon-Substrate Intracortical Microelectrode Arrays for Long-Term Recording of Neuronal Spike Activity in Cerebral Cortex," IEEE Transactions on Neural Systems and Rehabilitation Engineering, vol. 11, pp. 151-155, 2003.

19. R. Huang, C. Pang, Y.C. Tai, J. Emken, C. Ustun, R. Andersen, and J. Burdick, "Integrated parylene-cabled silicon probes for neural prosthetics," in Proc. MEMS 2008, Tucson, Arizona, 2008.

20. C. Veraart, C. Raftopoulos, J.T. Mortimer, J. Delbeke, D. Pins, G. Michaux, A. Vanlierde, S. Parrini, and M.C. Wanet-Defalque, "Visual sensations produced by optic nerve stimulation using an implanted self-sizing spiral cuff electrode," Brain Research, vol. 813, pp. 181-186, 1998. 145

21. T. Yagi, Y. Ito, H. Kanda, S. Tanaka, M. Watanabe, and Y. Uchikawa, "Hybrid retinal implant: fusion of engineering and neuroscience," Proceedings IEEE international Joint Conference on Neural Networks, vol. 4, pp. 382-385, 1999.

22. M.S. Humayun, E.d.J. Jr, J.D. Weiland, G. Dagnelie, S. Katona, R. Greenberg, and S. Suzuki, "Pattern electrical stimulation of the human retina," Vision Research, vol. 39, pp. 2569-2576, 1999.

23. S.Y. Kim, S. Sadda, J. Pearlman, M.S. Humayun, E.d. Jr, and W.R. Green, "Morphometric analysis of the macula in eyes with disciform age-realted macular degeneration," The Association for Research in Vision and Ophthalmology annual meeting, vol. 42, 2001.

24. E. Zrenner, A. Stett, S. Weiss, R.B. Aramant, E. Guenther, K. Kohler, K.-D. Miliczek, M.J. Seiler, and H. Haemmerle, "Can subretinalmicrophotodiodes successfully replace degenerated photoreceptors?," Vision Research, vol. 39, pp. 2555-2567, 1999.

25. A.Y. Chow, V.Y. Chow, K.H. Packo, J.S. Pollack, G.A. Peyman, and R. Schuchard, "The artificial silicon retinamicrochip for the treatment of vision loss from retinitis pigmentosa," Arch Ophthalmol, vol. 122, pp. 460-469, 2006.

26. M.S. Humayun, R. Propst, E.d. Jr, K. McCormick, and D. Hickingbotham, "Bipolar surface electrical stimulation of the vertebrate retina," Arch Ophthalmol, vol. 112, pp. 110-116, 1994.

27. M. Javaheri, D.S. Hahn, R.R. Lakhanpal, J.D. Weiland, and M.S. Humayun, "Retinal prostheses for the blind " Ann. Acad. Med., vol. 35, pp. 137-144, 2006.

28. J.D. Weiland and M.S. Humayun, "Visual prosthesis," Proceedings of the IEEE, vol. 96, pp. 1076-1084, 2008.

29. Y.C. Tai, L.S. Fan, and R.S. Muller, "IC-processed micro-motor: design, technolog, and testing," in Proc. IEEE Int. Conf. on Micro Electro Mechanical Systems, 1989, pp. 1-6.

30. K.A. Shaw, Z.L. Zhang, and N.C. Macdonald, "SCREAM-i-a single mask, singlecrystal silicon, reactive ion etching process for microelectromechanical structures," Sensor. Actuat. A-Phys., vol. 40, pp. 63-70, 1994.